Materials Letters 143 (2015) 212–214

Contents lists available at ScienceDirect

Materials Letters

journal homepage: www.elsevier.com/locate/matlet

UV–vis absorption shift of mixed valance state tungstate oxide: $Ca_{0.72}La_{0.28}WO_4$

Long Yuan [a], Jing Yu [b], Shan Wang [c], Keke Huang [a], Xiaoru Ren [a], Yu Sun [a], Xiaofeng Wu [a], Shouhua Feng [a,*]

[a] State Key Laboratory of Inorganic Synthesis and Preparative Chemistry, College of Chemistry, Jilin University, Changchun 130012, P.R. China
[b] Osakapaint Co., Ltd., West Gushan county, Jiangyin 214413, P.R. China
[c] Jilin Institute of Chemical Technology, The Department of Materials Science and Engineering, 45 Chengde Street, Jilin 132022, P.R. China

ARTICLE INFO

Article history:
Received 15 October 2014
Accepted 23 December 2014
Available online 2 January 2015

Keywords:
Microstructure
Particles
Nanosize
Nanocrystalline materials
Blue shift

ABSTRACT

$CaWO_4$ and $Ca_{0.72}La_{0.28}WO_4$ samples were synthesized via mild hydrothermal method at 180 °C. Composition, phase purity, morphology and W element binding energy were characterized by induced couple plasma atomic emission spectrum (ICP-AES), powder x-ray diffraction (XRD), scanning electron microscopy (SEM), x-ray energy dispersive spectroscopy (EDS), and x-ray photoelectron spectroscopy (XPS). UV–vis absorption spectroscopy shows absorption peak shift due to La^{3+} doping, which induced to the presence of mixed valence states of W^{5+} and W^{6+} in scheelite-type structure compound. Hence, blue shift of UV–vis absorption from 350 nm to 405 nm was observed in La^{3+}-doped calcium tungstate.

1. Introduction

The alkaline-earth tungstate family with a formula of AWO_4 ($A=Ca^{2+}$, Sr^{2+}, Ba^{2+}) has been well studied for its fascinating applications such as catalysis [1], Raman converter [2], nonlinear media for the transformation of the radiation wavelength in lasers [3], self-activating phosphor under UV or x-ray excitation [4], laser excited luminescence host [5] and electrical properties [6,7]. Structurally it crystallizes in $I4_1/a$ space group with four molecules in each crystallographic cell at ambient atmosphere. The divalent A^{2+} and hexavalent W^{6+} coordinate with eight and four O atoms, respectively, and both sites form S_4 symmetry [8]. Usually, two adjacent Ca^{2+} were tightly enclosed by their neighboring WO_4 tetrahedral orderly with strong bonds between the [–O–W–O–] with [–Ca–O–Ca–] clusters [9]. Several factors may induce the breaking of structural symmetry: large and small cations doping at the Ca-site, WO_4 tetrahedral distortion, and formation of oxygen vacancies. Many previous works concentrated on the photoluminescent properties of small rare-earth cation doped $CaWO_4$ such as Eu^{3+} and Tb^{3+} [10,11], which worked as activators for red emission in the crystal lattice. For the larger rare-earth cations, such as La^{3+}, only one paper has been reported the Czochralski method, which grows a La-doped $CaWO_4$ single crystal that increases crystal transparency and radiation hardness considerably [12]. In rare-earth doped $PbWO_4$, the luminescence intensity could be dramatically suppressed by La^{3+} occupying the Pb-site [13]. However, no report has been concerned on nano-particles of La-doped $CaWO_4$ material preparation, which may be because of the large lattice mismatch by inserting La^{3+} into the smaller Ca^{2+} sites. In general, the alkaline-earth tungstates are prepared by high temperature solid state reaction [14], solvothermal methods [15,16], spray pyrolysis method [17], sol–gel method [18], molten salt method [19], and co-precipitation method [20]. Among all these methods, the hydrothermal synthesis is a promising synthetic route because the synthesis can be well controlled through a lot of reaction parameters, such as the temperature, reaction time, pH, mineralizer and surfactant [21]. Moreover, the low reaction temperature and the liquid phase condition are preferential to grow a high-purity crystal with a low oxidation state [22]. Some pure phase of thermodynamically-unstable products (such as $Pr_3Fe_5O_{12}$ garnet) could only be prepared via the hydrothermal method because of the subcritical crystallization conditions [23]. In previous work, we found excellent bright red luminescence of $CaWO_4$ by Eu^{3+} and Mo^{6+} dopant [24]. In this work, we therefore report for the first time the hydrothermal synthesis of La^{3+} doped calcium tungstate ($Ca_{0.72}La_{0.28}WO_4$) nanoparticles in the presence of sodium borohydride as an effective reducing agent. $CaWO_4$ was also synthesized as a reference for UV–vis absorption shift as La^{3+} dopant.

2. Experimental

The synthesis of $CaWO_4$ and $Ca_{0.72}La_{0.28}WO_4$ were performed under mild hydrothermal conditions. Experimental details were as

* Corresponding author. Tel.: +86 431 85168661; fax: +86 431 85168624.
E-mail address: shfeng@jlu.edu.cn (S. Feng).

http://dx.doi.org/10.1016/j.matlet.2014.12.115
0167-577X/

follows: For $Ca_{0.72}La_{0.28}WO_4$, 1.4 mmol calcium chloride ($CaCl_2$) and 0.6 mmol lanthanum chloride ($LaCl_3$) were firstly dissolved in 10 mL deionized water to form a solution. Then, 2 mmol sodium tungstate ($Na_2WO_4.2H_2O$) and 0.1 g sodium borohydride ($NaBH_4 \cdot 2H_2O$) were added and stirred for 20 min. The suspension was transferred to a 15 mL Teflon-lined stainless steel autoclave with its filling capacity at 80% and was kept at 180 °C for 10 h. After the hydrothermal reaction, the autoclave was cooled to room temperature naturally. The product powders were collected, washed with distilled water and dried in air at 70 °C for 6 h. For the synthesis of $CaWO_4$, 2 mmol calcium chloride and 2 mmol sodium tungstate ($Na_2WO_4.2H_2O$) were dissolved in 10 mL deionized water on a stir plate at room temperature for 20 min, and the subsequent procedure was the same as the synthesis of $Ca_{0.72}La_{0.28}WO_4$.

Compositions of the samples were analyzed by inductively coupled plasma atomic emission spectroscopy (ICP-AES) technique on a Perkin-Elmer Optima 3300DV spectrometer (Sheldon, CT). Powder x-ray diffraction (XRD) analysis was carried out on a Rigaku D/Max 2500V/PC x-ray diffractometer (Tokyo, Japan) with monochromatic Cu Ka radiation (λ=0.1506 nm) and with a scanning speed of 1°/min of 2-theta degree range of 10–60° under the acceleration voltage of 50 kV and the acceleration current of 200 mA. Pawley refinements of the as-prepared samples were calculated with Accelrys Material Studio software. The particle size and morphology of the products were examined by field emission scanning electron microscopy (SEM) on Helios NanoLab 600I equipped with an x-ray energy dispersive spectroscopy (EDS), at an acceleration voltage of 10 kV. x-ray photoelectron spectrum (XPS) was acquired with Thermo ESCALAB 250 spectrometer (San Jose, CA, USA). UV–vis absorption spectra were investigated with a HITACHI U-4100 spectrometer (Tokoy, Japan).

3. Results and discussion

The elemental analyses of the as prepared $CaWO_4$ and $Ca_{0.72}La_{0.28}WO_4$ were determined by ICP-AES method. The molar ratios of Ca/W and Ca/La/W are 1/1 and 0.72/0.28/1.00 for the as-prepared two compounds, respectively. The molar ratios of Ca and La related to W element in samples are close to the start ratio of raw materials, where Ca/W=1/1 and Ca/La/W=0.7/0.3/1.0 for $CaWO_4$ and $Ca_{0.72}La_{0.28}WO_4$, respectively.

Fig. 1 shows the XRD patterns and Pawley refinements of $CaWO_4$ (a) and $Ca_{0.72}La_{0.28}WO_4$ (b). All of the diffraction peaks can be indexed in tetragonal *I41/A*, which is in accordance with the JCPDS card No. 41-1431. Observed (o) and calculated (line), as well as difference (bottom) profiles are shown. The Bragg reflection positions are marked with vertical bars. Schematic shows the scheelite structure of $CaWO_4$ viewing along *a*-axis (c) and relative atomic positions (d): white ball represent Ca, red ball O and green ball W. No traces of additional peaks from other phases were observed. The diffraction peaks for all the samples were significantly broadened, which is due to the small sizes of the as-obtained nano-particles. The unit cell parameters are $a=b=$ 5.2473 Å, $c=$11.3847 Å (Rp=5.53%) for $CaWO_4$ and $a=b=$5.2499 Å, $c=$11.3994 Å (Rp=4.49%) for $Ca_{0.72}La_{0.28}WO_4$. The crystal unit cell parameter sizes of *a*, *b* and *c* increased because of the larger radius of La^{3+} in the substituted crystallographic sites of Ca^{2+}. The crystal structure of $CaWO_4$ (top view along *a*-axis) was shown in Fig. 1(c); the WO_4 tetrahedral was separated by Ca^{2+} through a bridge O of Ca–O–W linkage. The bond length of W–O is 1.784 Å, which is much smaller than Ca–O bond (Fig. 1(d)), because of the high valance state and small ion size of W^{6+}.

Fig. 2 shows SEM and EDS patterns of $CaWO_4$ (a) and $Ca_{0.72}La_{0.28}WO_4$ (b). Their aggregation particles are composed of a large number of nano-crystallites. $CaWO_4$ sample exhibits a regular round sphere with diameters of about 20 μm, whereas $Ca_{0.72}La_{0.28}WO_4$ sample exhibits both coralloid sphere-like particles with diameters of about 8 μm decorated with many irregular particles. For $CaWO_4$, the EDS patterns show that the atomic ratio of Ca:W is about 1.1:1, which is close to the atomic ratio of Ca:W in $CaWO_4$ chemical formula. For $Ca_{0.72}La_{0.28}WO_4$, the EDS patterns indicate that the surface atomic ratio of Ca:La:W is about 0.70:0.28:1, which is close to the chemical formula of $Ca_{0.72}La_{0.28}WO_4$.

Fig. 3 shows XPS spectra of W elements in $CaWO_4$ (a) and $Ca_{0.72}La_{0.28}WO_4$ (b). In CaWO4 (Fig. 3(a)), W4f peaks positioned at 35.3 eV and 37.4 eV belong to the +6 oxidation state of W. In $Ca_{0.72}La_{0.28}WO_4$ (Fig. 3(b)), W 4f peaks positioned at 35.5 eV and 37.5 eV, which are slightly shifted to higher binding energy. The W 4f spectrum could be separated into two doublets of W^{6+} and W^{5+}. The first doublet has a W $4f_{7/2}$ line at 35.5 eV and a W $4f_{5/2}$ line at 37.6 eV W with a ΔE of 2.1 eV associated with the oxidation state W^{6+}. The second doublet has a binding energy with W $4f_{7/2}$ line at 33.8 eV and a W $4f_{5/2}$ line at 36.0 eV with a ΔE of 2.2 eV associated with W^{5+}. The changing of binding energy of W in $Ca_{0.72}La_{0.28}WO_4$ is because of the La^{3+} doping at the Ca^{2+}-site, which causes mixed valance state of W.

Fig. 4 shows UV–vis absorption spectra of $CaWO_4$ (a) and $Ca_{0.72}La_{0.28}WO_4$ (b). As it can be observed, the maximum absorption band of the $CaWO_4$ sample is at around 400 nm, while the maximum absorption band of $Ca_{0.72}La_{0.28}WO_4$ sample is shifted towards lower wavelength (blue shift) and has the maximum absorption band at around 350 nm. The observed blue shift in the absorption between La^{3+} doped sample and $CaWO_4$ is reasonable. First, the doping of La^{3+} reduces the size of unit crystal cell of the samples, and the corresponding reduced bond length generates the blue shift; Secondly, the doped La^{3+} ions come into the lattice of $CaWO_4$ and preferentially replace Ca^{2+} ions. The La^{3+} in the crystal lattice results in the increasing of the energy gap. The free electrons are more constrained in the valence band, and thus the electrons can be moved with difficulty to the excited state in the conduction band. As a result, the UV absorption band of La^{3+} doped $CaWO_4$ samples was shifted to lower wavelength.

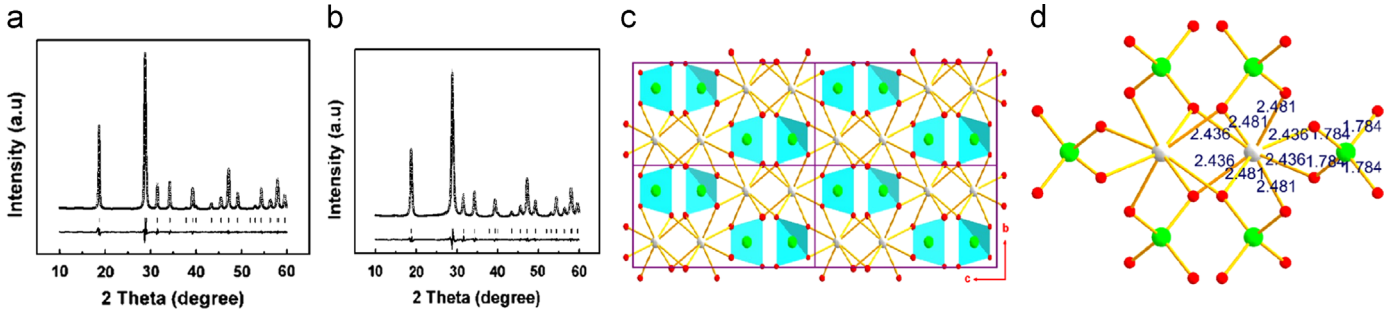

Fig. 1. Pawley refinement of $CaWO_4$ (a) and $Ca_{0.72}La_{0.28}WO_4$ (b) powders from XRD data. All peaks can be well indexed in Tetragonal *I41/A*. Observed (○), calculated (line), and difference (bottom) profiles are shown. The Bragg reflection positions are marked with vertical bars. Schematic show of the scheelite structure of $CaWO_4$ viewing along *a*-axis (c) and relative atomic positions (d): white ball represent Ca, red (black) ball O and green (grey) ball W.

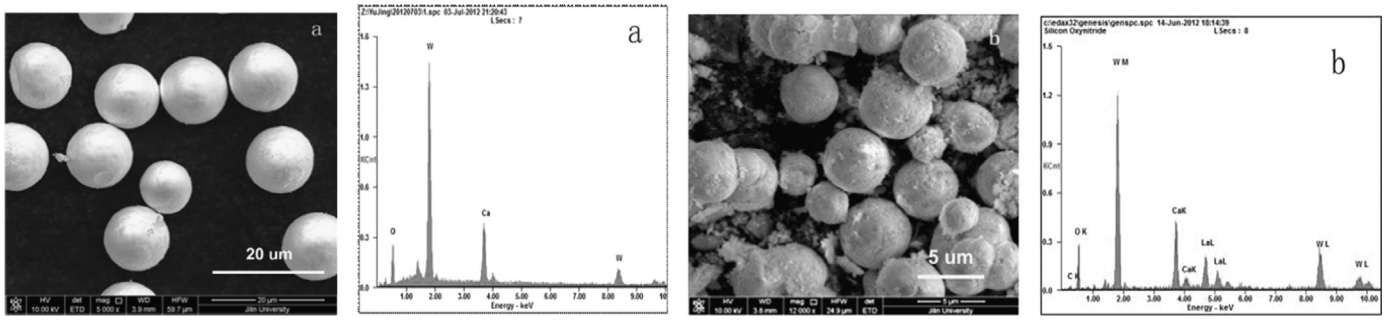

Fig. 2. SEM images and EDS spectra of $CaWO_4$ (a) and $Ca_{0.72}La_{0.28}WO_4$ (b) spheres.

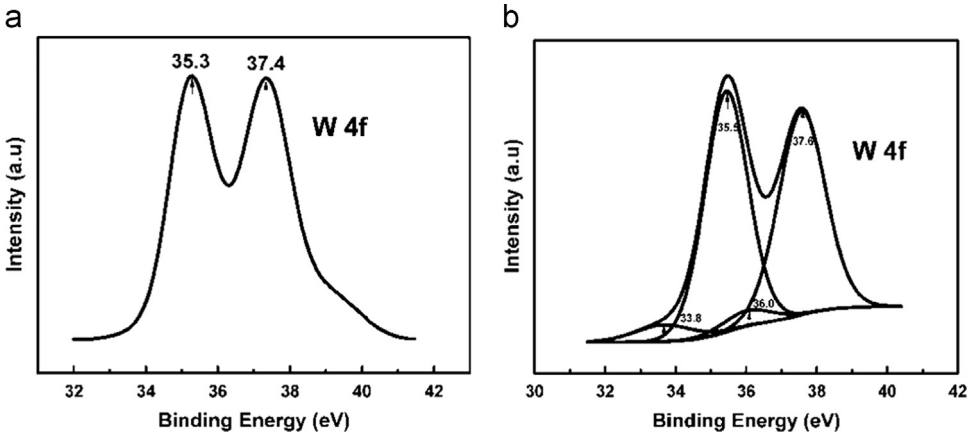

Fig. 3. XPS spectra of W from $CaWO_4$ (a) and $Ca_{0.72}La_{0.28}WO_4$ (b) samples.

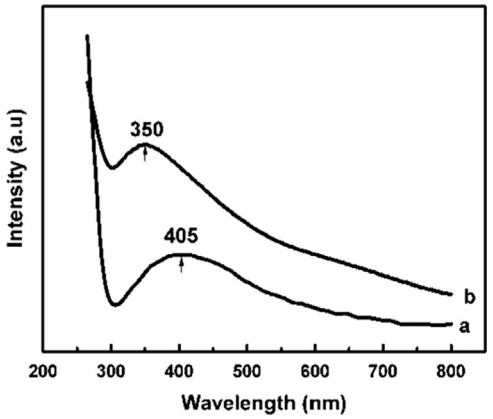

Fig. 4. UV–vis absorption spectra of $CaWO_4$ (a) and $Ca_{0.72}La_{0.28}WO_4$ (b) powders.

4. Conclusions

In summary, we have successfully synthesized coralloid sphere-like $Ca_{0.72}La_{0.28}WO_4$ by one-step hydrothermal route in sodium borohydride reducing environment. According to XRD and XPS analysis, $Ca_{0.72}La_{0.28}WO_4$ has a scheelite structure with W mixed valence states. UV–vis absorption spectroscopy results demonstrated a blue shift effect in La^{3+} doped $CaWO_4$.

Acknowledgments

The authors would like to acknowledge the National Natural Science Foundation of China for financial support (Nos. 90922034 and 21131002) and Specialized Research Fund for the Doctoral Program of Higher Education (No. 20110061130005). Thanks to Prof. Eric Handberg in East China Institute of Technology, Jiangxi Key Laboratory for Mass Spectrometry and Instrumentation for English improvement.

References

[1] Kim DS, Ostromecki M, Wachs IE. J Mol Cat A: Chem 1996;106:93–102.
[2] Cerny P, Jelinkova H, Zverev PG, Basiev TT. Prog Quantum Electron 2004;28:113–43.
[3] Basiev TT, Sobol AA, Voronko YK, Zverev PG. Opt Mater 2000;15:205–16.
[4] Thongtem T, Phuruangrat A, Thongtem S. Appl Surf Sci 2008;254:7581–5.
[5] Mikhailik VB, Kraus H, Wahl D, Itoh M, Koike M, Bailiff IK. Phys Rev B 2004;69:205110.
[6] Esaka T. Solid State Ionics 2000;136–137:1–9.
[7] Thangadurai V, Knittlmayer C, Weppner W. Mater Sci Eng B 2004;106:228–33.
[8] Gürman E, Daniels E, King JS. J Chem Phys 1971;55:1093–7.
[9] Cavalcante LS, Longo VM, Sczancoski JC, Almeida MAP, Batista AA, Varela JA, et al. CrystEngComm 2012;14:853–68.
[10] Chen YQ, Sung WP, Byung KM, Byung CC, Jung HJ, Guo CF. CrystEngComm 2013;15:8255–61.
[11] Enrico C, Philippe B, Rachid M, Marco B, Pieter D. Inorg Chem 2010;49:4916–21.
[12] Baccaro S, Bohacek P, Cecilia A, Laguta V, et al. Phys Stat Sol 2000;178:799–804.
[13] Huang YL, Zhu WL, Feng XQ, Man ZY. J Solid State Chem 2003;172:188–93.
[14] Parhi P, Karthik TN, Manivannan V. J Alloys Compd 2008;465:380–6.
[15] Hernandez-Sanchez BA, Boyle TJ, Pratt HD, et al. Chem Mater 2008;20:6643–56.
[16] Chen SJ, Li J, Chen XT, Hong JM, Xue ZL, You XZ. J Cryst Growth 2003;253:361–5.
[17] Lou ZD, Cocivera M. Mater Res Bull 2002;37:1573–82.
[18] Chamberland BL, Kafalas JA, Goodenough JB. Inorg Chem 1977;16:44–6.
[19] Wang YG, Ma JF, Tao JT, Zhu XY, Zhou J, Zhao ZQ, et al. Mater Lett 2006;60:291–3.
[20] Thongtem T, Kungwankunakorn S, Kuntalue B, et al. J Alloys Compd 2010;506:475–81.
[21] Feng SH, Xu RR. Acc Chem Res 2001;34(3):239–47.
[22] Feng SH, Yuan HM, Shi Z, Chen Y, et al. J Mater Sci 2008;43:2131–7.
[23] Guo L, Huang K, Chen Y, et al. J Solid State Chem 2011;184:1048–53.
[24] Yu J, Huang K, Yuan L, Feng S. New J Chem 2014;38:1441–5.